MECHANICAL PROPERTIES OF A 2618/ TiB_2 IN-SITU METAL MATRIX COMPOSITE

Christine Bartels, Lars Stegelmann, Mischa Crumbach, Günter Gottstein

Institut für Metallkunde und Metallphysik, RWTH Aachen, 52056 Aachen, Germany

ABSTRACT The mechanical properties of an in-situ processed 2618 (AlCu2Mg1.5Ni) based composite material reinforced with 5 vol. % TiB_2 particles were studied. Room temperature tensile tests were carried out on solution treated and quenched samples as well as on T6 treated samples. Furthermore, T6 treated samples were tested at elevated temperatures up to 350°C. To make the influence of the TiB_2 particles on the mechanical properties transparent, all experiments were also conducted on a non-reinforced 2618 reference material. The mechanical properties are interpreted in terms of microstructure changes due to the presence of the ceramic particles.

Keywords: *in-situ MMCs, particle reinforced MMCs, mechanical properties, microstructure, elevated temperatures*

1. INTRODUCTION

Recently, new in-situ processed metal matrix composites (MMCs) have attracted increasing attention. The composite material investigated in this study was produced using a melt-metallurgical in-situ process which offers a low cost processing route and allows to incorporate TiB_2 particles as reinforcement phase into an Aluminium matrix [1]. For further optimization and for an application of this new material it is important to understand how and by which mechanisms the TiB_2 particles alter the microstructure and the mechanical properties.

The mechanical properties were studied in tensile tests after a T6 heat treatment as well as directly after solution treatment and quenching. It is well known that particle reinforcement can have significant effects on the ageing behaviour of MMCs [2,3,4] like an accelerated ageing response and a less pronounced increase of hardness when compared to the respective non-reinforced alloy. So, when investigating an artificially aged state it is not possible to study only the influence of particles on the strength because this effect is often superimposed by the particles' influence on the ageing process. Therefore, additionally the solution treated state was studied. The tensile tests were accompanied by microstructure studies and texture measurements. All experiments were also conducted on a non-reinforced commercially produced 2618 alloy in order to extract the influence of the TiB_2 particles on the microstructure and thereby on the mechanical properties.

2. EXPERIMENTAL

The investigated 2618 + 5 vol. % TiB_2 composite material was produced by London and Scandinavian Metallurgical Co. Limited using a melt-metallurgical in-situ technique based on the reaction of the salts K_2TiF_6 and KBF_4 with an Aluminium melt [1]. The reaction results in a dispersion of small TiB_2 particles with an average diameter of about 1 µm in the melt. The material was directly chill cast and hot extruded to rods with a diameter of 38 mm (extrusion ratio 43, extrusion temperature 440°C). A commercially available hot extruded, non-reinforced 2618 alloy was used as reference alloy. All samples of both materials were solution treated for 1.5 h at 530°C in an air circulation furnace. One part of the samples was solution treated, quenched in ice water and stored at –18°C to

avoid precipitation before testing. The other part of the samples was quenched in cold water (T < 20°C) and artificially aged for 19 h at 190°C according to the conventional T6 treatment of the 2618 matrix alloy.

The tensile tests were conducted using a Zwick 1484 universal testing machine at a constant crosshead speed which corresponded to an initial strain rate of $6.6 \cdot 10^{-4}$ s^{-1}. For tests at elevated temperatures between 100°C and 350°C a tube furnace was used. The samples were heated to the respective testing temperature. Tensile tests were commenced after thermal equilibrium was attained, which took between 0.5 and 1.5 h. Using the tube furnace did not allow to measure elongation directly at the sample surface. Instead the elongation was determined with an inductive gauge fixed on top of the crosshead. From the measured total displacement the machine's elastic response was subtracted.

Texture measurements were carried out with an automated X-ray texture goniometer using Cu-K_α radiation.

3. RESULTS

3.1 Mechanical Properties

In table 1 the mechanical properties at ambient temperature of the non-reinforced 2618 alloy and the 2618 based MMC are compared after solution treatment and quenching and after a T6 heat treatment. The incorporation of 5 vol. % TiB_2 leads to an improvement of the yield stress $R_{p0.2}$ by 110 MPa in the solution treated and quenched state. The ultimate tensile strength R_m after solution treatment and quenching is improved for 67 MPa. In the T6 treated state the TiB_2 particles cause $R_{p0.2}$ to rise by 56 MPa whereas R_m increases only by 19 MPa. Furthermore, artificial ageing has a much stronger effect on the non-reinforced alloy than on the composite material. While for the alloy the magnitude $R_{p0.2}$ and R_m increase by 258 MPa and 106 MPa, respectively, due the ageing, they only rise by 204 MPa ($R_{p0.2}$) and 58 MPa (R_m) for the reinforced material.

Table 1: *Mechanical properties at ambient temperature after different thermal treatments*

Material	thermal treatment	$R_{p0.2}$/ MPa	R_m/ MPa
2618 non-reinforced	solution treated and quenched	101 ± 3	343
2618 + 5 vol. % TiB_2	solution treated and quenched	211 ± 3	410 ± 10
2618 non-reinforced	T6	359 ± 24	449 ± 4
2618 + 5 vol. % TiB_2	T6	415 ± 5	468 ± 14

In fig. 1 the temperature dependence of $R_{p0.2}$ and R_m is presented for the MMC as well as for the non-reinforced material. All samples were tested in the T6 state. The error bars mark the variation of the different measured values. Both materials show a significant loss of strength and a decreasing difference between R_m and $R_{p0.2}$ with increasing test temperature. At ambient temperature as well as elevated temperatures up to 200°C the strength of the composite material is significantly superior to that of the non-reinforced alloy. The massive loss of strength that the alloy exhibits at 150°C is not so pronounced for the composite. At this temperature the reinforced 2618 material still has the same yield strength as the non-reinforced material at ambient temperature. However, when the temperature exceeds 250°C the yield strength and the ultimate tensile strength of both materials tend to converge, and at about 330°C even a cross over is observed, i.e. the reinforced material behaves even softer than the non-reinforced material.

The increase of strength due to the incorporation of TiB_2 is accompanied by a loss of ductility of the

composite material at temperatures below 250°C (Fig.2). Qualitative differences between the temperature influence on the ductility of both materials can be observed. The non-reinforced alloy exhibits a local maximum of the elongation to fracture at 150°C, which correlates with the drop of strength at this temperature. A subsequent local minimum at 250°C is followed by a further increase.

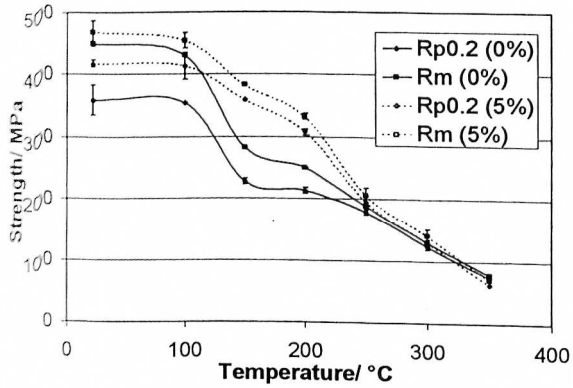

Fig. 1: *Temperature influence on yield strength ($R_{p0.2}$) and ultimate tensile strength (R_m) of the MMC 2618 + 5 vol. % TiB_2 and of the non-reinforced 2618 alloy, both after T6 heat treatment*

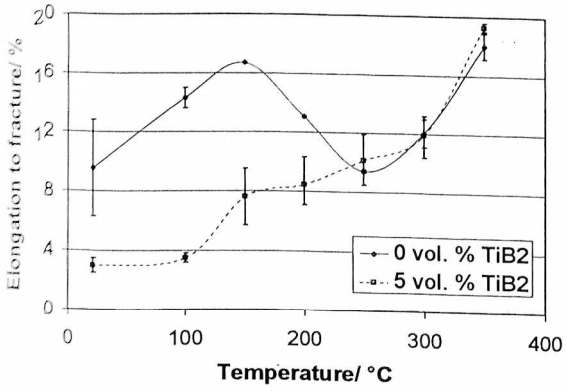

Fig. 2: *Temperature influence on the elongation to fracture of the MMC 2618 + 5 vol. % and of the non-reinforced 2618 alloy, both after T6 heat treatment*

In contrast the elongation to fracture of the MMC constantly rises with increasing temperature. At high temperatures a cross over of the elongation values is observed. The composite material becomes slightly more ductile than the non-reinforced alloy.

3.2 Microstructure

After extrusion the microstructures of the MMC exhibits a rather fine grain structure (Fig.3a). The alloy shows a diffuse fine substructure that is visible within some of the elongated grains (Fig. 3b). Intermetallic Al_9FeNi phases, which are present in both materials, are lined up along the extrusion direction. The TiB_2 particles in the MMC, which were originally located on the grain boundaries in the cast state, are also lined up along the extrusion direction. Both materials are characterized by <111> - <100> fibre textures typical of extrusion of fcc metals [5].

After the solution treatment hardly any microstructure changes are observed on the TiB_2 reinforced material. Only very few grains exhibit growth into the extrusion direction, but a large volume fraction remains unchanged. Also, the texture is not affected by the solution treatment. (Fig. 4a) The response of the non-reinforced alloy to the solution treatments is completely different.

Massive grain growth is observed which goes along with a significant change of the texture (Fig. 4b). The solution treated composite is characterized by a much smaller grain size than the non-reinforced 2618 alloy. In the non-reinforced alloy the average length of a grain in extrusion direction is 310 µm and the average width perpendicular to the extrusion direction is 180 µm.

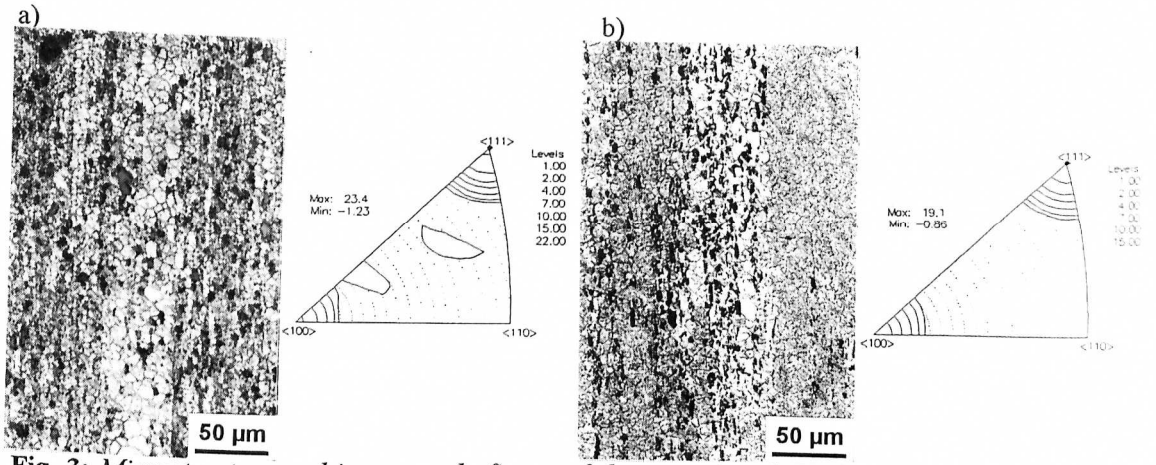

Fig. 3: *Microstructure and inverse pole figure of the extrusion direction of the 2618 + 5 vol. % TiB_2 composite (a) and of the non-reinforced 2618 alloy (b) after extrusion*

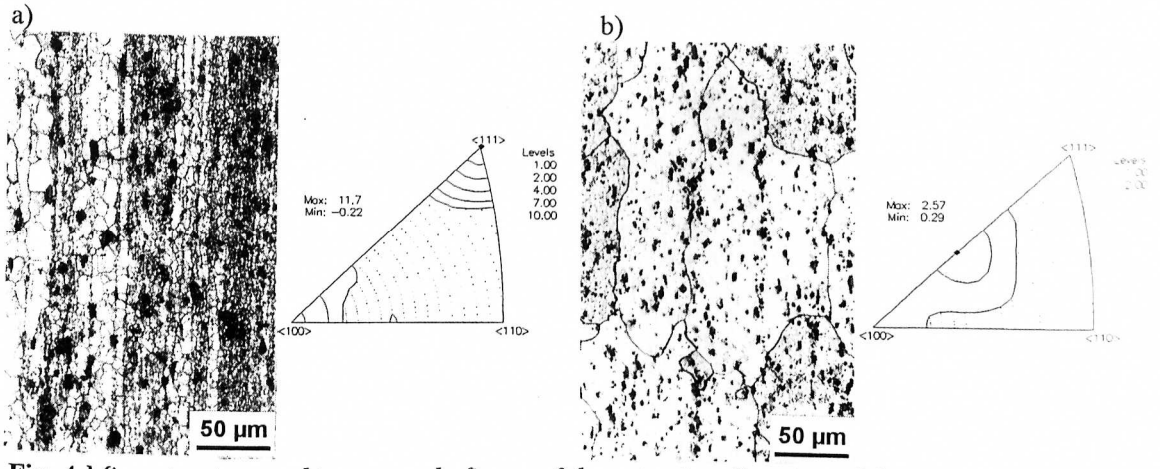

Fig. 4 *Microstructure and inverse pole figure of the extrusion direction of the 2618 +5 vol. % TiB_2 composite (a) and of the non-reinforced 2618 alloy (b) after solution treatment*

In contrast the average grain length and width in the composite is only 17 µm and 9 µm, respectively, in those areas in which only few TiB_2 particles are present. In areas with a higher TiB_2 content the grain size is even smaller. Single grain orientation measurements using the electron back scatter diffraction technique (EBSD) reveal that many of the grain boundaries in the composites are low angle grain boundaries. In contrast the grain boundaries visible in the non-reinforced alloy are high angle grain boundaries.

DISCUSSION AND CONCLUSION

The TiB_2 particles obviously affect the grain structure and the texture of the 2618 matrix after solution treatment. These two effects help to understand the differences in strength between the

composite and the alloy at the various temperatures and after the different thermal treatments.

The extrusion texture of the MMC is stabilized by the TiB_2 particles. This can be attributed to a suppression of primary recrystallization and subsequent grain growth. This hypothesis is supported by the high number of low-angle grain boundaries in the composite material, which is typical of a strong recovery process. In contrast the texture changes that are observed on the non-reinforced material during solution treatment indicate a recrystallization of this material. In order to evaluate the influence of the different textures on the strength of the two materials the measured macro-textures were decomposed into individual components. A Taylor simulation [6] was applied to the resulting set of orientations to determine the average Taylor factor for the two different textures. As second plastic criterion a random selection [7] was used. The results are given in table 2 for a full constraints [6] and for a relaxed constraints Taylor model [8]. Although the absolute values vary slightly depending on the type of model that is used, the values for the MMC are about 10 % – 15 % higher than those for the non-reinforced alloy.

Table 2: *Taylor factors calculated for the macro-textures of the 2618 alloy and the 2618 + 5 vol. % TiB_2 composite after solution treatment*

Material	Taylor Factor Full Constraints Taylor Model	Taylor Factor Relaxed Constraints Taylor Model
2618 solution treated	2.94	3.25
2618 + 8 wt. % TiB_2 solution treated	2.68	3.09

The macroscopic yield stress is related to the critical resolved shear stress according to Eq. 1.

$$\sigma = M_T \cdot \tau \qquad (1)$$

(σ: macroscopic yield stress, τ: critical resolved shear stress, M_T: Taylor factor)

Accordingly, a higher Taylor factor corresponds to a higher strength of the material, and the stabilization of the extrusion texture seems to be an important strengthening mechanism induced by the TiB_2 particles.

Moreover, the fine TiB_2 particles are assumed to directly interact with dislocations according to the Orowan mechanism. Thereby the critical resolved shear stress τ is increased. As the coefficients of thermal expansion (CTE) of TiB_2 and Al are very different (Al: $26.5 \cdot 10^{-6}$ K^{-1} [9], TiB_2: $7.7 \cdot 10^{-6}$ K^{-1} parallel to the c-axis, $4.1 \cdot 10^{-6}$ K^{-1} parallel to the a-axis [10]) it is very likely that thermally induced residual stresses lead to the generation of a high dislocation density [11]. This would result in an additional contribution to strength at moderate temperatures.

The small grain size of the composite material, too, contributes to the superior strength of the MMC at ambient temperature and at temperatures up to about 200°C. However, grain boundary diffusion and grain boundary sliding reduce high temperature strength in materials with a very fine grain structure. A transition from deformation solely by dislocation slip to deformation assisted by grain boundary diffusion and grain boundary sliding could account for the observation that the MMC behaves softer than the non-reinforced alloy at temperatures above 330°C. This also corresponds to the slightly superior elongation to fracture of the MMC at high temperatures.

Since the grain size as well as the texture of the MMC is not affected by the solution treatment, heating up to the test temperature will not change these microstructural features, too. However, high temperatures will cause dissolution and coagulation of the metastable S' precipitates which are responsible for the high strength of the 2618 alloy in the T6 state [3]. (Besides S' also θ' and X' phases can occur in addition.) When the efficiency of precipitation strengthening decreases, other

effects that limit the movement of dislocations gain importance. In the non-reinforced alloy the grain size is large, and the relatively coarse Al_9FeNi intermetallic phases have hardly any influence on dislocation glide. Furthermore, recrystallization during solution treatment leads to a low dislocation density. Hence, when the precipitation strengthening loses influence the average obstacle spacing for a moving dislocation in the non-reinforced alloy becomes very large. The MMC exhibits a much smaller grain size and additionally the TiB_2 particles, which are included in some of the larger grains, limit dislocation motion. Therefore, the effect of dissolution and coagulation of precipitates causes a stronger increase of the average obstacle spacing in the non-reinforced alloy than in the MMC and thereby probably the more pronounced loss of strength at 150°C.

This consideration also explains the observation that the particles lead to a much stronger increase of strength in the solution treated state than after T6 heat treatment, and make plausible that the ageing effect is more pronounced in the non-reinforced alloy. In the solution treated and quenched state the dislocations mainly interact with solute atoms, grain boundaries and non-dissolving second phase particles. So, in this state the average obstacle spacing for a moving dislocation is much higher in the non-reinforced alloy than in the TiB_2 reinforced composite. Therefore the formation of precipitates during ageing leads to a significant reduction of the obstacle spacing for a moving dislocations in the alloy. In contrast, the movement of a dislocation in the solution treated composite is already limited by a small grain size and by the spacing of TiB_2 particles. Thus it is expected that the reduction of the of the average obstacle spacing and the corresponding increase of strength are less pronounced for the MMC.

ACKNOWLEDGEMENT

This work is part of the Brite/ Euram Project „In-situ processing of Aluminium Matrix Composites" (ISPRAM). Financial support of the European Union is gratefully acknowledged.

REFERENCES

[1] P. Davies, J.L.F. Kellie, D.P. Parton: Patent WO 93/05189 (1993)
[2] S. Suresh, K.K. Chawla: Fundamentals of Metal Matrix Composites, editors: S. Suresh, A Mortensen, A. Needleman, Butterworth-Heinemann, Stoneham (1993), 119
[3] I.N.A. Oguocha, Y. Jin, S. Yannacopoulos: Mat. Sci. Techn., 13 (1997), 173
[4] C. Bartels, D. Raabe, G. Gottstein, U. Huber: Mat. Sci. Eng., A237 (1997), 12
[5] G. Wassermann, J. Grewen: Texturen metallischer Werkstoffe, Springer Verlag, Berlin (1962), 163
[6] G.I. Taylor: Journ. Inst. Met., 62 (1938), 307
[7] E. Arnoud, P. Van Houtte, T. Leffers: Materials Science and Technology, Vol. 6, editors R. W. Cahn, P. Haasen, E.J. Kramer, VCH (1993), 137
[8] H. Honeff, H. Mecking: Proc. 5th Int. Conf. On Textures Of Materials (ICOTOM 5), editors G. Gottstein, K. Lücke, Springer Verlag, Berlin (1978), 265
[9] C.J. Smithells, Smithells Metals Reference Book, 6th ed., editor: E. A. Brandes, Butterworths, London (1983), 14-3
[10] Thermophysical Properties of High Temperature Solid Materials, Vol. 6, editor: Y. S Touloukian, The Macmillan Company, New York, (1967), 244
[11] M. Taya, R.J. Arsenault: Metal Matrix Composites, Thermomechanical Properties, Pergamon Press, Oxford (1989), 52